Highlights of Spanish Astrophysics VII, Proceedings of the X Scientific Meeting of the Spanish Astronomical Society held on July 9 - 13, 2012, in Valencia, Spain. J. C. Guirado, L.M. Lara, V. Quilis, and J. Gorgas (eds.)

The atmospheric structure and fundamental parameters of the red supergiants AH Sco, UY Sct, and KW Sgr

B. Arroyo-Torres[1], M. Wittkowski[2], J. M. Marcaide[1], and P. H. Hauschildt[3]

[1] Departamento de Astronomía y Astrofísica, Universitat de València, C/Dr. Moliner 50, 46100, Burjassot, Spain
[2] ESO, Karl-Schwarzschild-St. 2, 85748, Garching bei München, Germany
[3] Hamburger Sternwarte, Gojenbergsweg 112, 21029, Hamburg, Germany

Abstract

We present the atmospheric structure and the fundamental parameters of the Red Supergiants (RSGs) AH Sco, UY Sct, and KW Sgr. We have carried out spectro-interferometric observations in the near-infrared bands (between 1.9 μm and 2.5 μm) with the VLTI/AMBER instrument in medium resolution. In the visibility data, we detect the presence of molecular layers of water and CO in extended atmospheres. For a uniform disk modelling, we observe size increases in the water band centered at 1.9 μm and in the CO band at 2.3–2.5 μm, with respect to the near-continuun bandpass (2.20 − 2.25 μm). Our near-infrared spectra of AH Sco, UY Sct, and KW Sgr are well reproduced by the PHOENIX model. However the synthetic visibility amplitudes of the model do not predict the large extensions of the molecular bands. The continuum (2.15 − 2.25 μm) appears free from contamination by molecular layers. Thus, the continuum fitting to the PHOENIX can be used to estimate the diameter. We estimate the Rosseland-mean photospheric angular diameter of AH Sco, UY Sct, and KW Sgr to be 6.12 ± 0.7 mas, 5.67 ± 0.55 mas, and 4.07 ± 0.65 mas, respectively (preliminary values). We estimate radii and effective temperatures, and place the stars in the HR diagram.

1 Introduction

Red supergiants (RSGs) are candidates for supernovae progenitors. They are in an evolved He-burning phase star and they have cold extensive atmospheres. Their atmospheric structure is not well understood yet. Our research may help to constrain the structure and morphology of the circumstellar environment close to the atmosphere and to obtain the fundamental parameters to locate the stars in the Hertzsprung-Russell (HR) diagram. The characterization and precise location of the RSGs in the HR diagram are of great importance to calibrate stellar evolutionary models for massive stars.

The fundamental parameters of RSGs are not well characterized yet. Recent broadband spectrophotometric observations compared to recent model atmospheres caused a dramatic revision of the location of RSGs in the HR diagram [9, 8]. A study of the extreme supergiant Betelgeuse [11] suggests the presence of extended CO layers, which can not be accounted for by classical hydrostatic model atmospheres. Other studies suggest the presence of water vapour layers in RSGs [12, 17].

2 Our observations

The Very Large Telescope Interferometer (VLTI) consists on the coherent combination of the four VLT Unit Telescopes (UT) and the four moveable 1.8 m Auxiliary Telescopes (AT). The telescopes can be combined in groups of two or three. After the light beams have passed through a complex system of mirrors and delay lines, the combination at near- and mid-infrared is performed by the instruments AMBER. AMBER (Astronomical Multi-BEam combineR) is an interferometric beam combiner for the VLTI working in the near-infrared (J, H, and K bands). It combines three beams coming from three telescopes. AMBER gives access to the visibilities of the object for three different spatial frequencies, one closure phase and spectroscopy information of the object. It works with three different spectral resolutions (R $\sim$ 30, R $\sim$ 1500, and R $\sim$ 12000).

We have observed AH Sco, UY Sct and KW Sgr with the VLTI, using three of the Auxiliary Telescopes. We have also used AMBER with an external fringe tracker FINITO [13]. We have used it with medium-resolution mode (R $\sim$ 1500) in the K-2.1 and K-2.3 bands (covering wavelengths between 1.9 μm and 2.5 μm).

Visibility and closure phase values were obtained from AMBER data using version 3.0.3b1 of the amdlib data reduction package [15, 1]. After that, using our scripts in IDL (Interactive Data Language), we performed the absolute wavelength, relative flux, and visibility calibration.

3 The PHOENIX model

We compare our data with synthetic data (model) to determine the angular diameter of our sources. We use the version 16.03 of the PHOENIX code (for a general description see [5]). This model uses a hydrostatic atmosphere, a local thermodynamic equilibrium (LTE) and a spherical geometry.

The modelling of atmospheres of cold giant stars, such as AH Sco, UY Sct, and KW Sgr, is complicated because of two reasons, the treatment of molecular opacities and the spherical extension of the atmospheres [6]. In the next section we discuss how the PHOENIX model fits our data.

The synthetic visibilities obtained for grids with high gravity do not show a high intensity for the CO bands (on the K-2.3 band). Since strong molecular bands of CO are present in our targets, the best grid for the data should be the one with low gravity. On the other hand, the effective temperatures, obtained from [16], for AH Sco and UY Sct are $T_{\rm eff} = 3574$ K, and for KW Sgr is $T_{\rm eff} = 3895$ K. Given these, we have decided to use a grid of the PHOENIX model with the following parameters: $T_{\rm eff} = 3600$ K, $\log(g) = 0.0$, $M = 20{\rm M}_{\odot}$, and solar metallicity for AH Sco; $T_{\rm eff} = 3200$ K, $\log(g) = 0.0$, $M = 20{\rm M}_{\odot}$, and solar metallicity for UY Sct; and $T_{\rm eff} = 3500$ K, $\log(g) = 0.0$, $M = 20{\rm M}_{\odot}$, and solar metallicity for KW Sgr. In the figure 1 the result of the fitting is shown (We only show the results of KW Sgr, but they are representative of all sources).

3.1 Results and atmospheric structure

Figure 1 shows normalized fluxes, squared visibility amplitudes and UD diameters (from top to bottom). In the graphics of the normalized flux and the squared visibility amplitudes (data in red) we also show the best fits of the PHOENIX models (blue). In the visibility curves, we can observe a maximum near 2.25 μm, and it decreases towards the water bands (centred at 1.9 μm) and the CO bands (2.3 μm to 2.5 μm). The decrease of the visibility indicates a contribution from extended emission from molecular layers of water and CO. In AH Sco and UY Sct we obtain similar results. These results prove the presence of molecular bands of H_2O and CO.

In the bottom of the Fig.1 the uniform disk diameter as a function of wavelength is shown. The curves present a minimum with a constant diameter at $2.20 - 2.25$ μm, and the diameter increases in the molecular bands H_2O band and the CO band. In the water band, the size increase is around 12% for KW Sgr (5% for AH Sco, and 20% for UY Sct) compared to the near-continuum bandpass, and in the CO band the size increase is around 30% for KW Sgr (20% for AH Sco, and 40% for UY Sct).

Previous studies had demonstrated that the near-infrared spectra of RSGs were reasonably well predicted by the PHOENIX model [7]. This is the case with our data too (figure 1). On the other hand, in the middle of figures 1, we can see that the PHOENIX model curve is very close to a UD model curve, and it does not predict the larger extensions of the molecular bands. These results likely indicate that the opacities from molecular bands are well implemented in the PHOENIX models, but the extension of the atmosphere is currently too compact in these models compared with our observations. This effect may be caused by missing pulsation, convection and/or wind acceleration in the models. Similar results for VY CMa have been obtained by [17].

4 Fundamental parameters

The measurements of the angular diameters in all bands are contaminated by the extended molecular layers, and thus the photospheric diameters are overestimated. However, with our spectral resolution , we can estimate the diameters only from the continuum ($2.20-2.25$ μm),

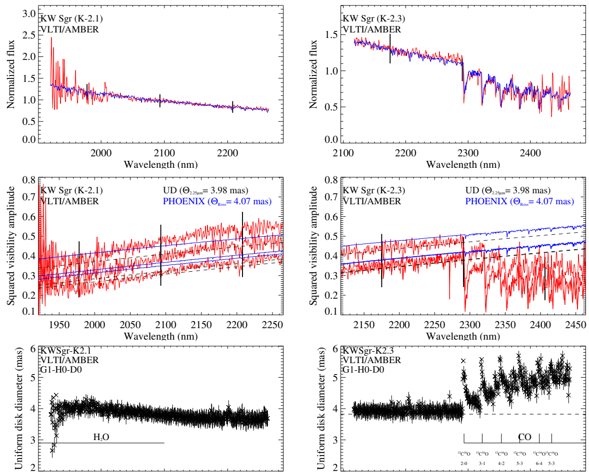

Figure 1: *Left panel:* Normalized flux, Squared visibility amplitudes and UD diameters (from top to bottom) of KW Sgr obtained with the MR-K 2.1 μm. *Right panel:* Same as left but obtained with MR-K 2.3 μm. As we can see in the top graphic the near-infrared spectra (red) is predicted reasonably well by the PHOENIX model (blue). But the models don't predict the visibility well (middle), the PHOENIX model curve (blue) is very close to a UD model curve (black). These results indicate that the opacities from molecular bands are well implement in the PHOENIX models, but the extension of the atmosphere is currently too compact compared with the observations. This may be caused by missing convection and/or pulsation in the models.

largely free from contamination by molecular layers. The diameters obtained with the best fits, using a UD model are $\theta_{UD} = (5.72 \pm 0.6)$ mas for AH Sco, (5.33 ± 0.55) mas for UY Sct, and (3.82 ± 0.6) mas for KW Sgr. Using the PHOENIX model, the Rosseland diameters estimated are $\theta_{Ross} = (6.12 \pm 0.7)$ mas, (5.67 ± 0.55) mas, and (4.07 ± 0.65) mas for AH Sco, UY Sct, and KW Sgr, respectively.

For estimating the effective temperature, we use the measured Rosseland angular diameters and a measurement of the bolometric flux. The luminosity is estimated from the bolometric flux and the distance. Table 1 summarizes the fundamental parameters for our targets.

Figure 2 shows the position of AH Sco, UY Sct, and KW Sgr in the Hertzsprung-Russell (HR) diagram together with the recent evolutionary tracks from [4]. Our targets are located close to the red limit of these tracks. AHSco and UYSct are close to the evolutionary track corresponding to an initial mass of 32 $M_\odot$, without rotation. KWSgr is close to the track with initial mass of 20 $M_\odot$, without rotation.

Table 1: Fundamental parameters of AHSco, UYSct, and KWSgr

Parameter	AHSco	UYSct	KWSgr
F_{bol} (10^{-9} W m^{-2})	2.15±0.32	1.45±0.22	0.97±0.15
d (pc)	2260±190 [2]	2900±317 [14]	2400±300 [10]
L 10^{32} W)	1.32±0.30	1.46±0.39	0.67±0.19
$\log(L/L_\odot)$	5.54±0.23	5.57±0.27	5.24±0.29
θ_{Ross} (mas)	6.12 ±0.7	5.67±0.55	4.07±0.65
$R(\mathrm{R}_\odot)$	1486±211	1767±258	1050±213
$T_{\rm eff}$ (K)	3625±248	3409±209	3639±321
$\log(T_{\rm eff})$	3.56±0.07	3.53±0.06	3.56±0.09

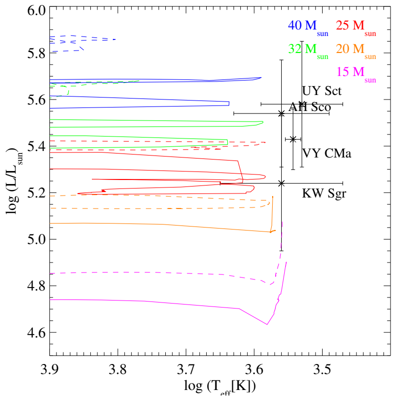

Figure 2: Location of AH Sco, UY Sct, KW Sgr (our work), and VY CMa [17] in the HR diagram using our fundamental parameters. It also shows the evolutionary tracks from [4] for masses of 15 M$_\odot$, 20 M$_\odot$, 25 M$_\odot$, 32 M$_\odot$ and 40 M$_\odot$. The solid lines are models without rotation, and the dashed lines are with rotation.

5 Conclusions

Our near-infrared spectra of AH Sco, UY Sct, and KW Sgr are well reproduced by the PHOENIX model. This likely indicates that the opacities from the molecular bands are well implemented. However the synthetic visibility amplitudes of the model do not predict the large extensions of the molecular bands (the PHOENIX model curve is very close to the UD model curve). This discrepancy may be caused by missing pulsation, wind acceleration and/or missing convection (our future work will focused in fitting our data to the 3D model by [3]). The continuum ($2.15-2.25$ μm) appears free from contamination by molecular layers. Thus, the PHOENIX model fitting can be used to estimate the diameter from this spectral region.

Using the PHOENIX model in the continuum, we estimate a Rosseland angular diameter of 6.12±0.7 mas ($R = (1486 \pm 211)\mathrm{R}_\odot$) for AH Sco, 5.67±0.55 mas (converting to a Rosseland radius of $R = (1767{\pm}258)\mathrm{R}_\odot$ for UY Sct, and 4.07±0.65 mas ($R = (1050{\pm}213)\mathrm{R}_\odot$) for KW Sgr. On the other hand, we observe low visibility amplitudes in the water and in the

CO bands. These lower amplitudes translate into larger sizes of our targets in these bands. Therefore we have evidence of a extended atmosphere with an envelope of molecular water and CO. Te position of the stars in the HR diagram falls close to the red limit of the tracks corresponding to stars of mass around 32 $M_\odot$ (AH Sco and UY Sct) or 25 $M_\odot$.

Acknowledgments

This work has been partially founded by grant AYA2009-13036-C02-02 of the Spanish MICINN, and by grant PROMETEO 104/2009 of the Generalitat Valenciana.

References

[1] Chelli, A., Utrera, O. H., & Duvert, G. 2009, A&A, 502, 705

[2] Chen, X. & Shen, Z.-Q. 2008, IAUS, 252, 247

[3] Chivassa, A., et al. 2011, A&A, 535, A22

[4] Ekstrom, S., Georgy, C., Eggenberger, P., et al. 2012, A&A, 537, 146

[5] Hauschildt, P. H. & Baron , E. 1999, J. Comp. Appl. Math, 109, 41

[6] Hauschildt, P. H., Allard, F., Ferguson, J., Baron, E., & Alexander, D. R. 1999, ApJ, 525, 871

[7] Lanon, A., Hauschildt, P. H., Ladjal, D., & Mouhcine, M. 2007, A&A, 468, 205

[8] Levesque, E. M., et al. 2009, AJ, 137, 4744

[9] Massey, P., Levesque, E. M., & Plez, B. 2006, ApJ, 646, 1203.

[10] Melnik, A. M. & Dambis, A. K. 2009, MNRAS, 400,518

[11] Ohnaka, K., Hofmann, K. H., Benisty, M., et al. 2009, A&A, 503, 183

[12] Perrin, G., Ridgway, S. T., Coudé du Foresto, V., et al. 2004, A&A, 418, 675

[13] Petrov, R. G., Malbet, F., Weigelt, G., et al. 2007, A&A, 464,1

[14] Sylvester, R. J., Skinner, C. J., & Barlow, M. J. 1998, MNRAS, 301, 1083

[15] Tatulli, E., Millour, F., Chelli, A., et al. 2007, A&A, 464, 29

[16] Van Loon, J. Th., Cioni, M. R. L., et al. 2005, A&A, 438, 273

[17] Wittkowski, M., Hauschildt, P. H., Arroyo-Torres, B., & Marcaide, J. M. 2012, A&A, 540, 12